# Conditional Methods for Continuum Reacting Flows in Porous Media

A.Y. Klimenko and M.M. Abdel-Jawad

*Mechanical Engineering Div., SoE, The University of Queensland, Qld 4072, Australia*
*ARC Centre for Functional Nanomaterials, SoE, The University of Queensland, Qld 4072, Australia*

**Published: Proc. of Comb. Inst., Vol. 31, 2007, pp. 2107-2115.**

**Abstract**

A special version of Conditional Moment Closure – PCMC – is suggested for modeling reacting flows in porous media. The model involves conditioning on a special tracer scalar, which is introduced to characterize scalar transport in the gaseous phase. (i.e. for the flow in the interparticle space or in the pores). The model accounts for interparticle variations of species concentrations and emulates diffusion in the interparticle space. Special boundary conditions that are consistent with conventional conditions at the phase interface are obtained for the PCMC model. The model is tested against complete direct simulation of a reacting flow in porous media with favourable results.

*Keywords:* CMC, heterogeneous reactions, porous media

## 1. Introduction

Contributions have been made to the study of flow in porous media for around 200 years [1]. Fundamental studies of flow have recieved rigorous mathematical attention (see for example [2]) and flow has been classified into the following main regimes depending on pore size and strength of adsorption: continuum (Poiseuille) flow, rarefied (Knudsen) flow, capillary force driven diffusion and surface diffusion (see for example [3]). The effects of pore structure and randomness on diffusion have also been studied (see for example [4]). Modern methods of treating reacting flows in porous media are also reviewed in ref. [5].In this work we focus on continuum flows with nonequilibrium chemical kinetics through porous media.

Continuum reacting flows in porous media are characterized by presence of two phases: the gaseous $\beta$-phase and the solid (or liquid) $\sigma$-phase [5]. Depending on application, the $\sigma$-phase can be represented by a material with extensive porous structure, rocks, particles or droplets. Chemical reactions are divided into two major groups: homogeneous reactions that occur in the volume occupied by the $\beta$-phase and heterogeneous reactions that occur on the surface separating the $\sigma$- and $\beta$-phases (the $\sigma/\beta$-interface). In this work, we are not primarily concerned with motion of the $\sigma$-phase and refer to the problem under consideration as a flow in porous media rather than a heterogeneous flow. In most conventional approaches, the reactions are treated with the use of averages over $\beta$-phase (i.e. the intrinsic averages [6, 7]). The alternative treatment [8] involves using solutions obtained for individual particles or droplets to characterize multiparticulate flow. Although the latter approach has an obvious restriction — the distributions of reacting species obtained for individual particles should not strongly interfere with each other — it points to that there could be significant variations of concentrations at smallest scales in the $\beta$-phase that makes the use of intrinsic averages inaccurate (although intrinsic averages still characterize the local fractions of reacting species better than superficial averages [5–7]). One can imagine a third, alternative treatment of reacting flows in porous media by resolving all details of the flow in pores or between the particles. Consid-

ering complexity of a typical porous media structure, the last approach seems to be more hypothetical than practical. Here, we call this approach "direct simulations" and distinguish it from modeling that is based on the use of various averages.

The goal of the present work is to follow the Conditional Methodology [9] and use conditional averages that characterize the interparticle scalar field much better than the intrinsic averages. The suggested model emulates scalar diffusion in interparticle space and, essentially, this model is a modification of Conditional Moment Closure (CMC) [9]. Note that in the present work the conditioning variable $Z$ is not the mixture fraction used in conventional CMC but a specially selected tracer scalar that, in $\beta$-phase, satisfies the scalar transport equation with a source term Generally, there is a certain degree of freedom in selecting the tracer scalar and its source term but, in the case of a good selection, the scalar $Z$ is, to a some extent, indicative of the distance from the closest $\sigma/\beta$-interface: we specify $Z = 0$ on the interface while $Z > 0$ in the $\beta$-phase. Special attention needs to be paid to formulation of the boundary conditions for CMC equations that should match the conventional conditions on the $\sigma/\beta$-interface. The suggested model is called PCMC – "Porous CMC".

In the present work, the PCMC model is tested against direct simulations. The direct simulations are preferred over experiments to ensure accurate control of reaction mechanisms that must be identical for the direct simulations and the model. The reaction mechanism and constants are selected in the most simple manner that can demonstrate the effect of change in a local concentration near the phase interface due to heterogeneous (surface) reactions. This effect can be modeled by PCMC but not by the conventional approaches based on intrinsic averages. This reaction mechanism involves two reactions, heterogeneous and homogeneous, and resembles one of the routes for char oxidation.

## 2. Conventional and conditional averaging in porous media

In the present work, we refer to three types of averaging that can be effectively used for modeling reacting flows in porous media: superficial, intrinsic and conditional [6, 7, 9]. These averages can be represented by the following equations

$$\langle Y \rangle = \int_{\infty} Y(\mathbf{x}^{\circ}) \Phi(\mathbf{x}^{\circ} - \mathbf{x}) d\mathbf{x}^{\circ} \qquad (1)$$

$$\overline{Y}_{\beta} = \frac{\langle Y\rho\beta \rangle}{\langle \rho\beta \rangle} = \frac{\langle Y\rho \rangle_{\beta}}{\langle \rho \rangle_{\beta}}, \;\; \langle \rho \rangle_{\beta} = \frac{\langle \rho\beta \rangle}{\langle \beta \rangle_{\beta}} \qquad (2)$$

$$\overline{Y}_{Z} = \frac{\langle Y\rho\beta | Z = Z^{\circ} \rangle}{\langle \rho\beta | Z = Z^{\circ} \rangle} \qquad (3)$$

where the angular brackets denote spatial averaging by evaluating a convolution integral with a bell-shaped weighting function $\Phi(x)$ that satisfies the normalization conditions

$$\int_{\infty} \Phi(\mathbf{x}) d\mathbf{x} = 1$$

The averaging is effectively performed only over the gaseous phase ($\beta$ -phase) and, generally, the variables $Y$ are not necessarily defined in the solid phase ($\sigma$ -phase). The function $\beta(x)$ is defined so that $\beta = 1$ in the $\beta$ -phase and $\beta = 0$ anywhere else. The superficial averages $\langle \cdot \rangle$ , the intrinsic averages $\langle \cdot \rangle_{\beta}$ , the intrinsic Favre (density-weighted) averages $\overline{(\cdot)}_{\beta}$ and the conditional Favre averages $\overline{(\cdot)}_{Z}$ can be consistently used not only for $\rho$ and $Y$ but also for other variables specifying conditions in the flow. The averaging $\langle \cdot | Z^{\circ} \rangle = \langle \cdot | Z = Z^{\circ} \rangle$ denotes conditioning on $Z = Z^{\circ}$ where $Z$ is a physical variable and $Z^{\circ}$ is the corresponding sample space variable. If $Z > 0$ only in the $\beta$ -phase (so that $Z = 0$ at the $\beta/\sigma$ phase interface) than the function $\beta$ can be omitted in the conditional averaging for any $Z^{\circ} > 0$ . In the rest of the paper $Z$ is presumed to satisfy these conditions

$$Z > 0 \text{ in } \beta\text{-phase and } (Z)_{\beta\sigma} = 0 \qquad (4)$$

With the use of the fine grained distribution function $\psi = \delta(Z - Z^{\circ})$ the conditional averaging equations take the form

$$\overline{Y}_{Z} = \frac{\langle Y\rho | Z^{\circ} \rangle}{\langle Y\rho | Z^{\circ} \rangle} = \frac{\langle Y\rho\psi \rangle}{\langle \rho \rangle_{\beta} P_z} \qquad (5)$$

where $P_Z$ is Favre (density-weighted) distribution function

$$P_z = \frac{\langle \rho\psi \rangle}{\langle \rho \rangle_{\beta}}, \;\; \int_{+0}^{\infty} P_Z(Z^{\circ}) dZ = 1 \qquad (6)$$

These averaging equations combine the techniques of using the phase indicator functions $\beta$ [6], the weighting function $\Phi(x)$ [7] and conditional averaging [9]. The convolution integral in Eq.(1) represents a spatial filtering operation rather than an ensemble average. However, if the characteristic distance between the particles $L_*$ is much smaller than the scale $L_f$, which characterizes the rate of change of the average parameters in the flow, and if the characteristic length scale $L_{\Phi}$ of the function $\Phi$ is selected so that $L_* \ll L_{\Phi} \ll L_f$, then filtering can be treated in the same way as averaging. In the rest of the paper, we do not need to distinguish $Z$ and $Z^{\circ}$; both of these values are denoted by $Z$.

## 3. Conditional equations

The definitions of superficial, intrinsic and conditional averages are general and not linked to a particular type of scalars although the scalars considered here are deemed to satisfy the continuity equation and

the scalar transport equation (at least within the $\beta$-phase)

$$\frac{\partial \rho}{\partial t} + \nabla\cdot(\rho \mathbf{u}) = 0 \tag{7}$$

$$\frac{\partial \rho Y_i}{\partial t} + \nabla\cdot(\rho \mathbf{u} Y_i) - \nabla\cdot(\rho D_i \nabla Y_i) = \rho W_i \tag{8}$$

where $Z \equiv Y_0$ is a tracer scalar representing the conditioning variable while $Y_1, Y_2, ...$ are the mass fraction of the reactive scalars. In addition to the volume reaction rate $W_i$, the reactive scalars are affected by the surface reactions (and, may be, adsorption) $S_i$ on the interface between the phases (the $\beta/\sigma$-interface).

With conventional conditional notation of $Q_i \equiv (\overline{Y_i})_Z$, the CMC equation takes the form [9]

$$\frac{\partial Q_i \langle\beta\rho\rangle P_Z}{\partial t} + \nabla\cdot(\langle\beta\rho\mathbf{u}Y_i|Z^\circ\rangle P_Z) = \overline{(W_i)}_Z \langle\beta\rho\rangle P_Z + \frac{\partial J_i}{\partial Z} \tag{9}$$

where

$$J_i \equiv -\overline{(W_i)}_Z \langle\beta\rho\rangle P_Z + \frac{D_i}{D_0}\overline{N}_Z \langle\beta\rho\rangle P_Z \frac{\partial Q_i}{dZ^\circ} - Q_i \frac{\partial \overline{N}_Z \langle\beta\rho\rangle P_Z}{\partial Z^\circ} + J_i' + E_i$$

$$J_i' \equiv \left\langle \beta\rho(D_0 + D_i)\nabla Y_i' \cdot \nabla Z | Z^\circ \right\rangle P_Z - \frac{\partial \langle\beta\rho N' Y_i' | Z^\circ\rangle P_Z}{\partial Z^\circ}$$

$$E_i \equiv \nabla\cdot(\rho D \nabla(Y_{,i}\psi)) + \nabla\cdot(\langle\beta\rho(D_i - D_0)\nabla Y_i | Z^\circ\rangle P_Z)$$

$N = D_0(\nabla Z)^2$ is the scalar dissipation and the "prime" superscript denotes the conditional fluctuations $Y_i' = Y_i - Q_i$ or the value of $J_i'$ which is linked to the conditional variations. We follow the CMC approach [9] and the terms $J_i'$ and $E_i$ are consistently neglected in the rest of the paper. The trivial case of $W_i = 0$ and $Y_i = 1$ substituted into Eq.(9) yields the pdf equation

$$\frac{\partial \langle\beta\rho\rangle P_Z}{\partial t} + \nabla\cdot(\overline{\mathbf{u}}_Z \langle\beta\rho\rangle P_Z) + \frac{\partial \overline{(W_0)}_Z \langle\beta\rho\rangle P_Z}{\partial Z} + \frac{\partial^2 \overline{N}_Z \langle\beta\rho\rangle P_Z}{\partial Z^2} = 0 \tag{10}$$

Here $\langle\beta\rho\rangle \equiv \langle\beta\rangle\langle\rho\rangle_\beta$ by definition. Using Eqs.(9) and (10) results and neglecting the transport by conditional velocity fluctuations $u'$ results in

$$\frac{\partial Q_i}{\partial t} + \overline{\mathbf{u}}_Z \cdot \nabla Q_i + \overline{(W_0)}_Z \frac{\partial Q_i}{\partial Z} = \overline{(W_i)}_Z + \frac{D_i}{D_0}\overline{N}_Z \frac{\partial^2 Q_i}{\partial Z^2} + \left(\frac{D_i}{D_0} - 1\right)\frac{1}{P_Z}\frac{\partial \overline{N}_Z P_Z}{\partial Z}\frac{\partial Q_i}{\partial Z} \tag{11}$$

## 4. Boundary conditions

The integrals of the conditional equations must be consistent with the superficial averages of the continuity and scalar transport equations that are obtained by multiplying Eqs.(7) and (8) by $\beta$ and averaging in accordance with the spatial averaging theorem [6, 7] formulated for an arbitrary vector $\mathbf{G}$

$$\nabla\cdot\langle\beta\mathbf{G}\rangle = \langle\beta\nabla\cdot\mathbf{G}\rangle + \langle\delta_{\beta\sigma}\mathbf{n}\cdot\mathbf{G}\rangle$$

After neglecting the large-scale (but not the small-scale) transport by molecular diffusion we obtain

$$\frac{\partial \langle\beta\rho\rangle}{\partial t} + \nabla\cdot\langle\beta\rho\mathbf{u}\rangle = M \tag{12}$$

$$\frac{\partial \langle\beta\rho Y_i\rangle}{\partial t} + \nabla\cdot\langle\beta\rho\mathbf{u}Y_i\rangle = \langle\beta\rho W_i\rangle + F_i \tag{13}$$

where $M = \langle m\delta_{\beta\sigma}\rangle$ is the average mass flux into the $\beta$-phase, $m = \rho(u - s)\cdot\mathbf{n}$ is the local mass flux relative to the phase interface, $\delta_{\beta\sigma}\mathbf{n} = \nabla\beta$ is the Delta-function evaluated at the phase interface (note that the subscript "$\beta\sigma$" indicates values evaluated on the $\beta$-side of the surface while the subscript "$\sigma\beta$" denotes values evaluated on the $\sigma$-side; these values may differ from each other), $\partial\beta/\partial t = -\delta_{\beta\sigma}s\cdot\mathbf{n}$ and

$$F_i \equiv \langle Y_i m\delta_{\beta\sigma}\rangle - \langle\rho D_i\nabla Y_i\cdot\mathbf{n}\delta_{\beta\sigma}\rangle = \langle mY_i\delta_{\sigma\beta}\rangle + \langle S_i\delta_{\sigma\beta}\rangle \tag{14}$$

is the average flux of scalar $Y_i$ into the $\beta$-phase. Although these equations are formally applicable to conditions when $\sigma$-phase is represented by particles which are allowed to move (fluidized beds, for example), this case would need additional equations specifying transport of the $\sigma$-phase and is not specifically considered here.

The integral of Eq. (9) and the zeroth and the first moments of the pdf equation (10) — all these equations are integrated over the $\beta$-phase region ($+0 < Z < \infty$) — are consistent with Eqs. (12) and (13) provided that

$$\langle\beta\rho\rangle\left(\frac{\partial \overline{N}_Z P_Z}{\partial Z} + \overline{(W_0)}_Z P_Z\right)_{\beta\sigma} = M \tag{15}$$

$$\langle\beta\rho\rangle\left(\overline{N}_Z P_Z\right)_{\beta\sigma} = -F_0 = \langle\rho D_0\nabla Z\cdot\mathbf{n}\delta_{\beta\sigma}\rangle \tag{16}$$

$$M\left((Q_i)_{\beta\sigma} - (Q_i)_{\sigma\beta}\right) - \left(\frac{D_i}{D_0}N_Z\langle\beta\rho\rangle P_Z\frac{\partial Q_i}{\partial Z}\right)_{\beta\sigma} = A\langle S_i\rangle_{\beta\sigma} \tag{17}$$

where $A = \langle\delta_{\sigma\beta}\rangle$ is the average phase interface surface per unit volume. In these equations we consistently replace the local values by the conditional averages. According to the CMC logic, the reaction source terms are evaluated as

$$\overline{(W_i)}_Z = W_i(Q_1, Q_2, ...), \tag{18}$$

$$\langle S_i \rangle_{\beta\sigma} = S_i \left( (Q_1)_{\beta\sigma}, (Q_2)_{\beta\sigma}, ... \right) \qquad (19)$$

## 5. PCMC model for the test case

In this section we introduce simplified equations that are suitable for modeling the test case presented in the following section. The phase interface mass flow is small and neglected $M = 0$ (this corresponds to a relatively slow consumption of the $\sigma$-phase). The diffusion coefficients were selected constants and equal to each other and kinematic viscosity $D_0 = D_i = \nu$ — these values are denoted in the rest of the paper by $D = \text{const}$. The flow is presumed stationary $\partial/\partial t = 0$ with the average velocity directed along axis $y$. The density $\rho$ and porosity $\langle\beta\rangle$ remain constant. Here and in the rest of the paper, the values are normalized by characteristic distance between particles $L_*$ and by a certain characteristic time $\tau_*$: $x^* = x/L_*$, $y^* = y/L_*$, $u^* = u\tau_*/L_*$, $D^* = D\tau_*/L_*^2$. The scalar value $Z$ is normalized by its mean: $Z^* = Z/\overline{Z}_\beta$ (i.e. $\overline{Z^*}_\beta = 1$). $W_0^* = W_0/\overline{Z}_\beta$ and $N^* = N\tau_*/\overline{Z}_\beta^2$. The scale $\tau_*$ is selected so that $D^* = 1$, although we still keep $D^*$ in the equations for the sake of transparency. The distribution function is normalized to preserve unity of its integral over $Z^*$ (compare to Eq.(6)): $P_Z^* = P_Z\overline{Z}_\beta$. The reactive scalars are normalized as $Q_i^* = Q_i\rho\mu_i^{-1}C_*^{-1}$ where $\mu_i$ is the molar mass of component $i$ and $C_*$ is a characteristic molar concentration specified in the next section. The same normalization applies to $Y^*$. The source terms are normalized as $W_i^* = W_i\tau_*\rho\mu_i^{-1}C_*^{-1}$ and $S_i^* = S_i\tau_*L_*^{-1}\mu_i^{-1}C_*^{-1}$ while $A^* = AL_*$ is the normalized surface to volume ratio and $F_0^* = -F_0/(\overline{Z}_\beta\rho) > 0$ is the normalized sink of the tracer scalar $Z$.

Special attention needs to be paid to the proper selection of the tracer scalar $Z$ that, effectively, characterizes location in the interparticle space. If $W_0 = 0$ the scalar mean value $\overline{Z}_\beta = \overline{Z}_\beta(y)$ decreases exponentially with $y$ in the direction of the mean flow due to absorption of the scalar on the phase interface. The scalar $\xi = Z/\overline{Z}_\beta(y)$ is not conservative and can be used as a tracer scalar. We found, however, that the scalar $\xi$ has variations whose scale is noticeably larger than $L_*$; hence this scalar is not suitable to characterize the flow in the interparticle space. The scalar with a constant $W_0$ ($W_0 = \text{const}$ in the $\beta$-phase and $W_0 = 0$ in $\sigma$-phase) appears to be much better suitable as a tracer scalar characterizing local distances from the phase interface. After a short transitional region, the field $Z$ becomes developed and $\overline{Z}_\beta$ becomes constant. The value of the constant $W_0$ is not important since the scalar $Z$ can always be normalized by this constant.

Assuming that the tracer scalar field ($Z$-field) is developed, the convective terms in Eq.(10) disappear and this equation can be integrated using the boundary condition in Eq.(15) for $M = 0$. The system of normalized conditional equations takes the form

$$W_0^* P_Z^* + \frac{\partial \overline{N}_Z^* P_Z^*}{\partial Z^*} = 0 \qquad (20)$$

$$\overline{u}_Z^* \frac{\partial Q_i^*}{\partial y^*} + W_0^* \frac{\partial Q_i^*}{\partial Z^*} =$$

$$W_i^*(Q_1^*, Q_2^*, ...) + \overline{N}_Z^* \frac{\partial^2 Q_i^*}{\partial (Z^*)^2} \qquad (21)$$

while the boundary conditions (17) and (16) are now written as

$$-\left( \overline{N}_Z^* P_Z^* \frac{\partial Q_i^*}{\partial Z^*} \right)_{+0} = \frac{A^*}{\langle\beta\rangle} S_i^* \left( (Q_1^*)_{+0}, ... \right) \qquad (22)$$

$$\langle\beta\rangle \left( \overline{N}_Z P_Z \right)_{+0} = F_0^* = \langle\beta\rangle W_0^* \qquad (23)$$

$$\overline{N}_\beta^* = W_0^* \overline{Z}_\beta^* \qquad (24)$$

The subscript "$+0$" denotes values taken at the limit of $Z^* \to +0$ corresponding to the $\beta$-side of the phase interface; this subscript is essentially the same as "$\beta\sigma$" but emphasizes its explicit link to the variable $Z^*$. The right-hand side of Eq.(23) is obtained by integrating Eq.(20) over $Z^*$ while Eq.(24) is obtained by evaluating the first moment of Eq.(20). The surface to volume ratio is linked to the conditional characteristics by the equation

$$\frac{A^*}{\langle\beta\rangle} = \left( P_Z^* \left( \frac{\overline{N}_Z^*}{D^*} \right)^{1/2} \right)_{+0}. \qquad (25)$$

while integrating of Eq.(20) yields the following formula for $P_Z^*$

$$P_Z^* = \frac{W_0^*}{\overline{N}_Z^*} \exp\left( -\int_0^{Z^*} \frac{W_0^*}{\overline{N}_Z^*} dZ^* \right) \qquad (26)$$

We note that the equation for intrinsic averages can be obtained by integrating PCMC equation (21) multiplied by $P_Z^*$ and taking into account Eqs.(20) and (22)

$$\frac{\partial \overline{(u^* Y_i^*)}_\beta}{\partial y^*} = \overline{(W_i^*)}_\beta + \frac{A^*}{\langle\beta\rangle} \overline{(S_i^*)}_\beta \qquad (27)$$

The conventional models operate with intrinsic averages; hence decoupling the $u$-$Y$ correlation and approximating the reaction source terms in terms of $\overline{(Y_i^*)}_\beta$ results in

$$\overline{u}_\beta^* \frac{\partial \overline{(Y_i^*)}_\beta}{\partial y^*} = \overline{(W_i^*)}_\beta + \frac{A^*}{\langle\beta\rangle} \overline{(S_i^*)}_\beta \qquad (28)$$

$$\overline{(W_i^*)}_\beta = W_i^*(\overline{(Y_1^*)}_\beta, \overline{(Y_2^*)}_\beta, ...) \qquad (29)$$

$$\overline{(S_i^*)}_\beta = S_i^*(\overline{(Y_1^*)}_\beta, \overline{(Y_2^*)}_\beta, ...) \qquad (30)$$

Note that the major difference between the conventional and conditional models is mainly due to differences in approximating the reaction source terms – only the intrinsic averages (but not the conditional averages) of the reacting species are available to the conventional model.

## 6. Test case and grid generation

In order to test the PCMC model, we conducted direct simulations for a generic kinetic mechanism with four scalars, one surface reaction and one volume reaction. The reaction rates are selected to examine a wide range of the Damkoehler numbers. The reactions resemble one of the routes for carbon oxidation and, for the sake of transparency and without loss of generality, we use this interpretation of the reaction mechanism:

$$\text{R1: } \mathrm{C} + \mathrm{O} \rightarrow \mathrm{CO} \tag{31}$$

$$\text{R2: } \mathrm{CO} + \mathrm{O} \rightarrow \mathrm{CO_2} \tag{32}$$

The surface reaction R1 interacts with the volume reaction R2 and, depending on the reaction rates and conditions in the flow, may produce different percentage of CO and $CO_2$. The porous section of the computational domain is shown in Fig. 1. Although this domain is two-dimensional, it is quite complex and simulation of the reacting flow within this domain requires extensive calculations. A special Matlab code involving random generators was written for particle allocation. Python script was used to generate curves for particles at the locations, and with the dimensions specified by the random code generator. The remaining commands were completed manually to generate the domain with unstructured grids for this 2-D geometry using the commercial package CFD-GEOM (ESI Software) typically used in conjunction with the commercially available finite volume flow solver CFD-ACE.

Grids were controlled in GEOM using curvature resolution (in number of nodes per revolution), transition factor and maximum and minimum cell sizes. For a typical domain, these values were 30 degrees,1.1,3.7 and 0.000371 respectively for a domain size of 20 x 30 and resulting in approximately 20000 nodes and 35000 cells for the shown domain. The left and right sides of the domain were prescribed as periodic, the bottom boundary condition prescribed as a fixed velocity inlet while the top boundary condition prescribed as a fixed pressure outlet. The numerical accuracy of simulations was tested by control runs on a coarse grid with 5000 nodes and on a refined grid with extensive 40000 nodes that produced consistent results. A smaller domain or fewer particles in the domain would not allow for a reasonable evaluation of the conditional averages while having a smaller number of grid points would cause severe problems in resolving the interparticle space. The domain is periodic in horizontal direction and the average direction of the flow is upwards. Simulation convergence of a single run took up to several days. Although the domain seems quite complex, its complexity is limited compared to the extent and complexity of a real porous media. The particles are distributed randomly within the domain and the case shown in the figure has the porosity $\langle\beta\rangle = 0.75$. Atomic oxygen is present at the inlet (the bottom boundary of the domain) and reacts on the surfaces of the char particles forming CO followed by a fraction of CO being oxidized further into $CO_2$. The reactions persist until oxygen disappears from the flow. The normalizing value $C_* = 0.004$ mol/m$^3$ is selected to represent the inlet value of the inlet value of $C_{\mathrm{O}}$. (This concentration is small so that, practically, the density and temperature remain constant and the flowing gas is dominated by $N_2$). The products CO and $CO_2$ are not present at the flow inlet.

The rates for the reactions are conventionaly represented by

$$\text{R1: } S^*_{\mathrm{CO}} = k^*_1 Q^*_{\mathrm{O}} \tag{33}$$

$$\text{R2: } W^*_{\mathrm{CO_2}} = k^*_2 Q^*_{\mathrm{O}} Q^*_{\mathrm{CO}} \tag{34}$$

The normalized reaction coefficients are related to the conventional reaction coefficients $k_1$ and $k_2$ whose definition is based on molar concentrations of the reacting species by $k_1 = k^*_1/\tau_*$ and $k_2 = k^*_2/(C_*\tau_*)$.

The scalar $Z$ was introduced into direct simulations as a passive scalar that does not affect the reactions. The initial conditions were selected to make the transition to the developed field as short as possible. The PCMC model coefficients can be approximated by the following equations

$$\overline{N}^*_Z = N^*_0 \exp\left(-\frac{Z^*}{Z^*_N}\right), \;\; \overline{u}^*_Z = \frac{\overline{u}^*_\beta}{\overline{Z}^*_\beta} Z^* \tag{35}$$

so that $P^*_Z$ is determined from Eq.(26) as

$$P^*_Z = \frac{1}{Z^*_N} P^\circ_z(z, z_N), \;\; z \equiv \frac{Z^*}{Z^*_N}, \;\; z_N \equiv Z^*_N \frac{W^*_0}{N^*_0} \tag{36}$$

where

$$P^\circ_z(z, z_N) = z_N \exp\left(z + z_N(1 - \exp\left(z\right))\right) \tag{37}$$

The intrinsic mean value of $Z^*$ is linked to the parameter $z_N$ by the equation

$$\overline{Z}^*_\beta = Z^*_N \,\mathrm{Ei}_1(z_N) \exp(z_N) \tag{38}$$

These approximations of $\overline{N}^*_Z$, $\overline{u}^*_Z$ and $P^*_Z$ are consistent with each other and produce a reasonable match to the corresponding conditional parameters determined from the direct simulations as shown in Fig.2. The parameter $Z^*_N$ was set to $0.59$ to match the shape of $\overline{N}^*_Z$ determined from the simulations. The first point falls below the curve due to limited resolution of the gradients in the simulations. The parameter $N^*_0$ is selected to match $\overline{N}^*_\beta = 15$ which, according to (24), is the same as $W^*_0$ due to $\overline{Z}^*_\beta = 1$. The value of $z_N = 0.15$ is found form Eq.(38) determines that $N^*_0 = 59$ corresponds to $W^*_0 = 15$ in Eq.(36).

The matching curve for $\overline{N}_Z^*$ passes a bit below the simulated points to compensate the average for the difference in matching the first point. The intrinsic mean value of the velocity is $\overline{u}_\beta^* = 5.8$. For large values of $Z^*$ that have a low probability, $\overline{u}_Z^*$ become more close to a constant but this effect is neglected here and, as it can be seen in Fig.2, the linear approximation provides a good overall approximation for the conditional velocity. Note that the conditional velocity satisfies the boundary condition $\overline{u}_Z^* \to 0$ as $Z^* \to +0$. The calculated function $P_Z^*$ determined form Eqs.(26)-(37) is shown in Fig.2 to produce a reasonable match to the simulated $P_Z^*$. The area per the $\beta$-phase volume is $A^*/\langle\beta\rangle \approx 2$ in the domain shown in Fig.1. This value is matched well by the right-hand side of Eq.(25) with $\overline{N}_Z^*$ and $P_Z^*$ taken from both simulated and approximating curves in Fig.2.

The grid has a regular structure and calculating the conditional averages and the distribution function using the grid points would produce a biased statistics. The conditional averages evaluated by distributing the sampling points in the domain (uniformly and randomly) and interpolating the values from grid point into the sampling points. To avoid any problems with sampling, 1 000 000 sampling points were used in the evaluation of conditional averages so that the domain resolution and size but not the number of sampling points are the factors limiting the accuracy.

## 7. The results

In all of the calculations presented here, oxygen is fully consumed at the upper boundary of the porous domain. The fractions are normalized so that the value of $Y_{\rm O}^* + Y_{\rm CO}^* + Y_{\rm CO_2}^*/2 = 1$ in the domain. If oxygen is fully consumed then $Y_{\rm CO}^* + Y_{\rm CO_2}^*/2 = 1$. The value of $Y_{\rm CO}^*$ specifies the fraction of oxygen conversion into CO so that $Y_{\rm CO}^* = 1$ corresponds to the full conversion of oxygen into CO and $Y_{\rm CO}^* = 0$ corresponds to full conversion of oxygen into $CO_2$. The reaction rate constants are selected in terms of the Damkoehler number $\mathrm{Da}$

$$k_1^* = \frac{\langle\beta\rangle}{A^*}\overline{N}_\beta^*\,\mathrm{Da}, \quad k_1^* = \overline{N}_\beta^*\,\mathrm{Da} \tag{39}$$

Figure 3 presents the final (outlet) value of

$$\langle Y_{\rm CO}^*\rangle_\beta = \overline{(Y_{\rm CO}^*)}_\beta = \int_{+0}^{\infty} Q_{\rm CO}^* P_Z^* dZ \tag{40}$$

obtained by simulations and modeling as a function of $\mathrm{Da}$. The range of $\mathrm{Da}$ used in simulations is limited by resolution requirements for large $\mathrm{Da}$ and by incompleteness of the reactions within the calculation domain when $\mathrm{Da}$ is small. As expected, the conventional method (28)-(30) does not demonstrate any dependence on $\mathrm{Da}$ since, for this method $\overline{(Y_{\rm CO}^*)}_\beta$ depends only on the ratio $k_1^*/k_2^*$ that remains constant in Eq.(39). If $\mathrm{Da}$ is small, the reactive concentrations do not change significantly in the space between particles and, as expected, the conventional and conditional model yield the same results. As $\mathrm{Da}$ increases, the concentration of oxygen near the phase interface becomes smaller compared to its intrinsic average and, since CO is produced only near the phase interface, this decreases production of CO compared to production of $CO_2$. This effect is clear in the simulation and is well-reproduced by PCMC but not by the conventional model based on the intrinsic averages.

The comparison demonstrated in Fig.3 is indirect: simulations and modeling are compared in terms of the results they produce. Since the tracer passive scalar $Z$ is introduced in simulations, it is possible to evaluate the conditional expectations of the reactive scalars in simulations and make a direct comparison with $Q_i^*$ modeled by PCMC . We should note that the tracer scalar field becomes developed only at $y^* \gtrsim 2$ and, thus, the direct comparison is possible only for $y^* \gtrsim 2$. If $\mathrm{Da}$ is moderate, oxygen is not consumed and reactions still persist at $y^* \sim 2$. Figure 4 demonstrates the conditional expectations evaluated for $y^* = 2$ and $\mathrm{Da} = 0.4$. The PCMC model correctly predicts the tendencies observed in simulations.

## 8. Discussion

The PCMC model is a relatively computationally inexpensive model that, nevertheless, can characterize interparticle variations of the concentrations of reacting species. This model can be recommended to be used any time that the $\mathrm{Da}$ number is large enough (i.e. the reactions are fast enough) to cause noticeable variations of the concentration of species within the interparticle space (or in pores). If the $\mathrm{Da}$ number is sufficiently small, PCMC results would be similar to that of the conventional methods based on intrinsic averages. The tracer scalar $Z$ with $W_0$ that remains constant in the interparticle space seems to be a very good choice for the conditioning variable. The PCMC model (21) requires reasonable approximations for its coefficients, $\overline{u}_Z^*$ and $\overline{N}_Z^*$. While the linear approximation of $\overline{u}_Z^*$ in Eq.(35) (or, may be a linear approximation with a restricted maximal value) is likely to be applicable to a wide range of flows in porous media, the same is not assured for $\overline{N}_Z^*$. Approximation of $\overline{N}_Z^*$ and the corresponding approximation for $P_Z^*$ that is linked to $\overline{N}_Z^*$ by Eq.(20) may be dependent on structure of the pores. Ideally, passive simulations for the tracer scalar field $Z$ in a relatively small volume sampling the porous media under consideration should be performed first to find $\overline{u}_Z^*$ and $\overline{N}_Z^*$ – this task, although not trivial, is much easier than complete direct simulation of the whole reacting flow in a large volume of porous media. As information about the coefficients $\overline{u}_Z^*$ and $\overline{N}_Z^*$ is accumulated, the sampling simulations of the tracer field will not be needed for porous media with known properties.

The scaling of the dissipation with the pores size is another question of practical importance. In the

present simulations, normalization is based on distance between particles $L_*$ resulted in relatively high value of $\overline{N}^*_\beta \sim 15$. If the average radius of the particles $R \sim 0.3L_*$ is selected for normalization then $\overline{N}_\beta \sim 15D\overline{Z}^2_\beta/L^2_* \sim 1.5D\overline{Z}^2_\beta/R^2$. Hence, with the characteristic diffusion time $\tau_d \sim cR^2/D$ and the characteristic chemical time $\tau_c \sim \langle\beta\rangle A^{-1}k_1^{-1}$, we can estimate the Damkoehler number as $\mathrm{Da} \sim \tau_d/\tau_c \sim cR^2/(D\tau_c)$ where the exact value of the constant $c \sim 1$ depends on exact choice of $R$ and structure of the pores.

## 9. Conclusions

A new version of the CMC model – PCMC – , which is formulated for modeling of reactions in porous media, has been suggested. The PCMC model operates with mass fractions of reactive species conditioned on a given value of a tracer scalar and can be suitable for various kinetic mechanisms. The tracer scalar $Z$ is selected to characterize the local distance from the phase interface so that $Z = 0$ corresponds to the location at the phase interface. The boundary conditions that are consistent with the conditions on the phase interface are obtained for the PCMC model. Unlike the conventional models, the PCMC model can deal with closely packed or interacting particles (small pores) and at the same time emulate diffusion in the interparticle space. Comparison of the model against direct simulations demonstrate that, as expected, PCMC is capable of adequately simulating variations of concentrations of species that are neglected in conventional models based on intrinsic averages. Practically, the PCMC model is needed when the Damkoehler number representing the ratio of characteristic interparticle diffusion time and characteristic chemical time is not small.

## Acknowledgments

This work is supported by the Australian Research Council and by LINC Energy Ltd.

## References

[1] M. Kaviany, *Principles of Heat Transfer in Porous Media*, 1st Edition, Springer-Verlag, 1991.

[2] R. M. Barrer, *Diffusion in and Through Solids*, 2nd Edition, Cambridge University Press, 1951.

[3] A. J. Burggraaf, *Fundamentals of Inorganic Membrane Science and Technology*, 1st Edition, Cambridge University Press, 1996.

[4] M. M. Mezedur, M. Kaviany, W. Moore, *AIChE Journal* 48 (2002) 15–24.

[5] P. C. Lichtner, C. I. Steefel, E. H. Oelkers, *Reactive Transport in Porous Media*, Reviews in Mineralogy, vol 34, , Miner. Soc. of Amer., 1996.

[6] W. G. Gray, P. C. Y. Lee, *Int. J. Multiphase Flow* 3 (1977) 333–340.

[7] M. Quintard, S. Whitaker, *Transport Porous Media* 14 (1994) 163–177.

[8] F. A. Williams, *Combustion Theory*, 2nd Edition, Addison-Wesley, 1985.

[9] A. Y. Klimenko, R. W. Bilger, *Prog. Energy Combust. Sci.* 25 (1999) 595–687.

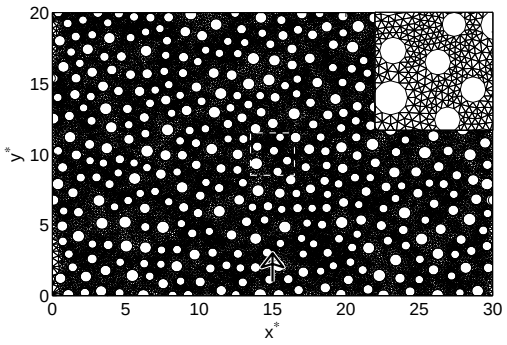


Fig. 1: Porous section of the computational domain. The insert in the right top corner enlarges the outlined region in the center. The arrow shows the direction of the mean flow.

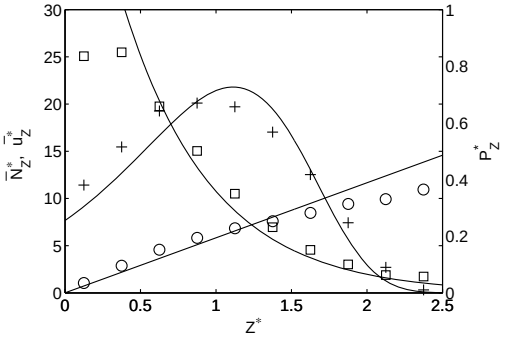


Fig. 2: The coefficients of PCMC model. Obtained from direct simulations: o – $\overline{u}^*_Z$; □ – $\overline{N}^*_Z$; + – $P^*_Z$. The same values approximated by Eqs. (35)-(37) are shown as solid lines.

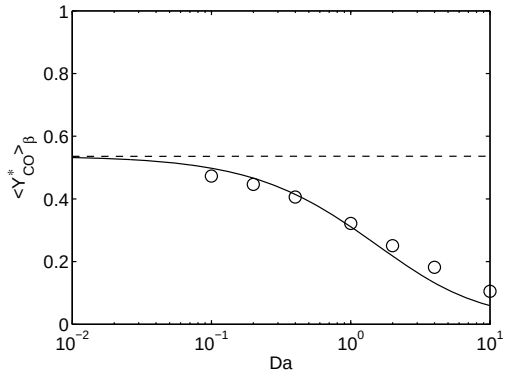


Fig. 3: CO fraction at the outlet for the range of Damkoler numbers. Conventional model - - - - -; PCMC ——; simulated values o.

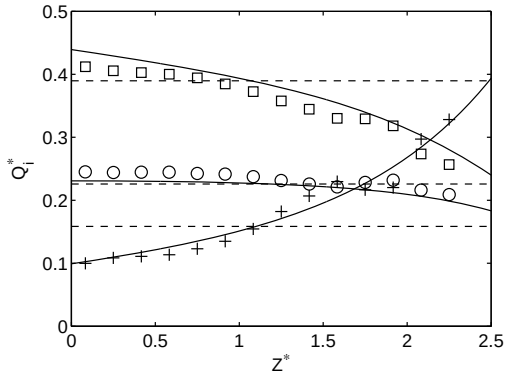


Fig. 4: Conditional expectations of reactive scalars at $y^* = 2$ and $\mathrm{Da} = 0.4$. Directly simulated: + – O; □ – CO; o – $CO_2$. The same values modelled by PCMC (——) and conventionally (- - - - -).